

Study of Epoxy Toughened by *In Situ* Formed Rubber Nanoparticles

Jun Ma,¹ Mao-Song Mo,² Xu-Sheng Du,² Shao-Rong Dai,² Ian Luck³

¹School of Advanced Manufacturing & Mechanical Engineering and Mawson Institute, University of South Australia, SA 5095, Australia

²Centre for Advanced Materials Technology, School of Aerospace, Mechanical and Mechatronic Engineering, The University of Sydney, NSW 2006, Australia

³School of Chemistry, The University of Sydney, NSW 2006, Australia

Received 28 September 2007; accepted 11 December 2007

DOI 10.1002/app.27882

Published online 9 July 2008 in Wiley InterScience (www.interscience.wiley.com).

ABSTRACT: The effect of rubber nanoparticles on mechanical properties and fracture toughness was investigated. Rubber nanoparticles of 2–3 nm were *in situ* synthesized in epoxy taking advantage of the reaction of an oligomer diamine with epoxy. The chemical reaction was verified by gel permeation chromatography (GPC) and ¹HNMR, and the microstructure was characterized by transmission electron microscope. The rubber nanoparticles caused much less Young's modulus deterioration but toughened epoxy to a similar degree in comparison with their peer liquid rubber that formed microscale particles during curing. Fifteen wt % of rubber nanoparticles increased fracture energy from 140 to 840 J/m² with

Young's modulus loss from 2.85 to 2.49 GPa. The toughening mechanism might be the stress relaxation of the matrix epoxy leading to larger plastic work absorbed at the crack tip; there is no particle cavitation or deformation; neither crack deflection nor particle bridging were observed. The compound containing rubber nanoparticles demonstrates Newtonian liquid behavior with increasing shear rate; it shows lower initial viscosity at low shear rate than neat epoxy; this provides supplementary evidence to NMR and GPC result. © 2008 Wiley Periodicals, Inc. *J Appl Polym Sci* 110: 304–312, 2008

Key words: nanocomposite; epoxy; toughen; rubber

INTRODUCTION

Epoxy resin is a widely used material across a range of industries. Epoxy is naturally brittle, which makes it vulnerable to flaws, in particular, microcracks, and thus limits its application. Sultan et al.¹ were among the first researchers to toughen epoxy by the incorporation of rubber spheres of ~ 1 μm diameter. Since their initial research, extensive investigations have been conducted for toughening epoxy (see the reviews of Refs. 2–4). A number of tougheners explored for toughening epoxy include liquid rubbers,^{5,6} thermoplastics,^{7,8} copolymers,^{9,10} silica nanoparticles,¹¹ silicate layers,^{12,13} core shell particles,¹⁴ and combinations of these.^{15,16} Clay can toughen epoxy 50–100% in fracture toughness, but it decreases both tensile strength and elongation at break.¹² Rigid polymer cannot toughen epoxy highly.^{7,8} Dendritic hyperbranched polymers were synthesized by “star & arm” skills and can form “core-shell” like structure,¹⁷ but the toughness improvement is not significant. Rubber particles, less rigid than the epoxy matrix, can induce the formation of microvoids which

is subsequently accompanied by the activation of yielding processes due to the reduction of the local yield stress, i.e., the plastic resistance of the material. In this case, a substantial amount of energy is dissipated within the plastic zone near the crack tip. Rubber toughening, however, is at the expense of matrix modulus.

It is noteworthy that the conventional rubber particles in epoxy are on microscale. Nanomaterials have attracted extensive interests in recently years. A special characteristic of nanoparticle is the high-specific surface area; this leads to the creation of a large portion of interface in the composite. Generally, the surface-to-volume ratio of particles increases with decreasing particle size. On the nanoscale the fraction of atoms localized at the surface per unit of volume is much higher than on the microscale. Therefore, the physical properties of particles for the same material are different on the nanoscale, and they may even be dominated by quantum mechanical effects. Both the toughness and strength of structural ceramics can be raised strongly, if nanoparticles instead of microparticles are used as building blocks.¹⁸ Furthermore, the interactions between nanoparticles and the epoxy matrix, depending on the particles' surface structure, geometry, and surface chemistry, have a great influence on the formation of the interface. Hence, a hypothesis is made—epoxy containing rubber nanoparticles may demon-

Correspondence to: J. Ma (jun.ma@unisa.edu.au).

Contract grant sponsor: Australian Research Council (ARC).

strate high fracture toughness but without (or with a little) decrease of Young's modulus. Thus, optically clear, ultimate tough, amorphous epoxy systems could be made. The author's recent research¹⁹ shows that epoxy can be toughened and strengthened simultaneously by inorganic spherical particles of 20–30 nm in diameter, which demonstrates completely different toughening mechanisms to their peer micron-size particles.

In this research, we will first *in situ* synthesis rubber nanoparticles in epoxy, and then study the mechanical properties, fracture toughness, and rheology of the epoxy/rubber nanocomposites. The tensile properties and fracture toughness will be compared with convention epoxy/rubber composites fabricated by Xiao and Ye²⁰ who used the same raw materials, processing and testing method as ours in this study.

EXPERIMENTAL

Materials

Epoxy resin diglycidyl ether of bisphenol A (DGEBA, Araldite-F) with epoxide equivalent weight 182–196 g/equiv was supplied by Ciba-Geigy, Australia. Piperidine hardener was ordered from Aldrich. Jeffamine D2000, used to *in situ* form rubber nanoparticles, was kindly provided by Huntsman (Singapore).

In situ synthesis of the rubber nanoparticles in epoxy

We previously prepared epoxy/rubber nanocomposites by directly mixing epoxy with rubber precursor, which yielded a nanoparticle-agglomerated morphology.²¹ So in this study we have an improved preparation technique as below.

One hundred gram of epoxy resin was mixed with 50 g acetone in a three-necked round-bottom flask equipped with a condenser. The mixture was stirred at 60°C for 10 min with a mechanical mixer, and then a desired amount of Jeffamine D2000 dissolved in acetone (50 wt %) was dropped into the flask by a micropump at 1 drop per second. The mixing continued for 30 min after all Jeffamine D2000 dropped in. Then the condenser was removed and the temperature increased to 120°C, at which the mixing continued for 2 h.

Curing of the nanocomposite

Epoxy resin was mixed with the hardener piperidine at 120°C for 5 min at a weight ratio of 100/5 (epoxy/hardener). Then the mixture was degassed, poured into various moulds for mechanical and toughness test followed by curing at 130°C for 17.5 h.

Gel permeation chromatography

A Waters chromatograph system with a 510 HPLC pump was used to measure the molecular weight of the polyurea, with a mixed-bed Styragel/HT 6E column and high-purity THF (Unichrom) eluent at a flow rate of 0.8 mL/min. Eluted fractions were detected with an R401 differential refractometer. Solutions for GPC were made up in THF (Aldrich).

¹H NMR

NMR spectra were recorded on a Bruker DPX400 NMR spectrometer, equipped with a 5 mm inverse probehead. The resonance frequency for ¹H was 400.13 MHz. Samples were prepared in deuterated chloroform and the spectra referenced to internal solvent residue (δ , 7.26). Sample temperatures were stabilized using a variable temperature unit (BVT2000), and spectra were recorded at 300 K. 64×10^3 data points were collected with 64 accumulated scans, over 8000 Hz, using a 90° (5.5 μ s) excitation pulse and a relaxation delay between scans of 2 s.

Rheology

For the rheology study, the steady shear measurements were conducted on a Paar Physica MCR 301 controlled stress rheometer, using a cone-plate measuring system. The geometrical sizes of the cone plate were 50 mm in diameter and 1° in cone angle. Prior to any test, the zero-gap between the cone plate and the plate was calibrated at 100°C. In the measurements, the sample was placed between the preheated plates and 3 min were allowed to reach thermal equilibrium at 100°C. The range of shear rate was set from 0.01 to 100 s⁻¹. For Jeffamine D2000, the shear rate range was set from 1 to 100 s⁻¹ because of the low viscosity.

Fracture toughness test

A rubber mold for compact tension (CT) and pins were prepared according to ISO 13586, with a specimen width $W \sim 30$ mm and thickness $B \sim 5.5$ mm. The thickness was chosen so as to meet the plane strain criterion. The CT samples were cured in the mold and then both sides were polished by emery paper until all visible marks disappeared. A sufficiently sharp crack was introduced to the sample by razor blade tapping. Tapping a razor blade on thermoset specimen initiates two types of cracks: non-propagated or instantly propagated cracks. Only the instantly propagated cracks are sufficiently sharp for fracture toughness test.²² Six specimens were tested for each set of data with a crosshead speed of 5 mm/min. The K_{1c} and G_{1c} values were calculated according to ISO13586.

Tensile test

Tensile dumb-bell samples with a gauge length of 50 mm were made using a silicone rubber mold and both sides were polished by emery paper until all visible marks disappeared. Then the samples were postcured at 120°C for 60 min. Tensile tests were performed at a strain rate of 5 mm/min at room temperature using an Instron 5567 tensile machine. An Instron extensometer 2630-100 was used to collect accurate displacement data to measure the modulus.

Morphology analysis

Ultra-thin sections ranging around 30 nm in thickness were cryogenically cut with a diamond knife in liquid nitrogen at -150°C using a Leica Ultracut S microtome. Sections were collected on 400-mesh copper grids and carefully stained with ruthenium tetroxide (RuO_4) vapor to enhance the phase contrast between the nanoparticle and the epoxy matrix. Subsequently, the thin sections were examined using a Philips CM12 transmission electron microscope at an accelerating voltage of 120 kV.

Microstructure of crack tips and the damage zone

Single-edge-double-notch-4-point specimen (SEDN-4PB) was widely employed to investigate toughening mechanisms.²³ SEDN-4PB geometry requires preparing nearly identical cracks on one side; under loading, one crack breaks and the other is in a critical state and propagates in an unstable manner. Similar to fracture toughness test, a sufficiently sharp crack is a prerequisite for fracture toughness mechanism investigation. Our experience shows that only an instantly propagated crack is sufficiently sharp and reproducible²²; it is impossible to initiate two nearly identical propagated cracks by tapping on a brittle thermoset SEDN-4PB. Therefore, we explored the following method for toughening mechanism identification.

The fracture toughness (K_{1c}) of target material was measured first. An instantly propagated crack was tapped on a new CT of the material. With the measured K_{1c} , the crack length and the sample size, we calculated the critical load for propagating the crack. Then this specimen was mounted on an Instron and loaded until 80% of the critical load (such a percentage load is called a subcritical load). The block containing the arrested crack tip was cut and subsequently trimmed to the middle section followed by a rectangular mesa trimming using a microtome. The procedure is shown in Figure 1. Ultrathin sections were carefully cut at 0.1 mm/s with a diamond knife using a Leica Ultracut S microtome. Then the sec-

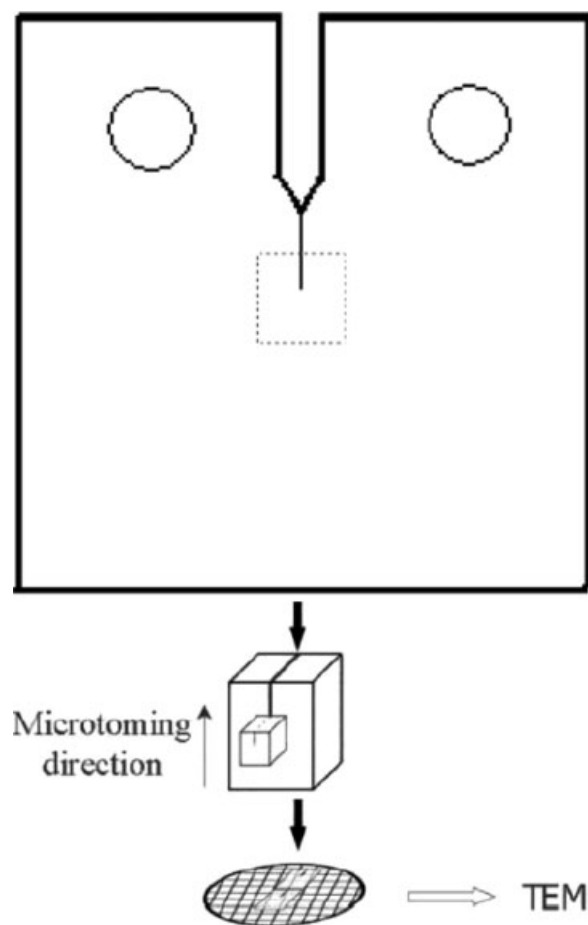


Figure 1 Scheme of optical microscope sampling processes at the crack tip.

tions were collected on 400-mesh copper grids and examined using a CM12 transmission electron microscope at an accelerating voltage of 120 kV.

Optical microscopy analysis

A section thin enough to transmit light was required for optical microscopy (OM). We prepared thin sections by petrographic polishing.²⁴ Sections taken from the deformed CT were potted in a room-temperature curing epoxy. These samples were then roughly ground, finely ground, roughly polished, and then finely polished. The polished surface was then mounted on to a clean glass slide using an optically clear epoxy. The sample and slide were allowed to cure overnight at room temperature. Excess materials were removed using a bend saw and the sample was again ground and polished until the plane of interest was finally reached. Useful thin sections ranged around 40- μm thick. All samples were viewed using a Nikon microscope using crossed-polarized light. A quarter wave plate was used to enhance the contrast of the birefringent regions.

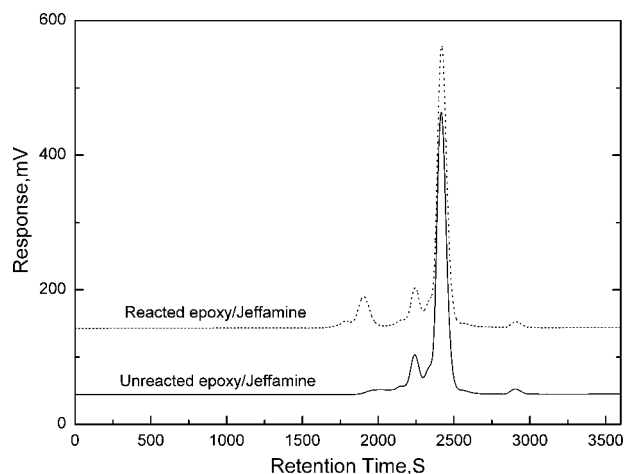


Figure 2 GPC chromatographs of unreacted epoxy/Jeffamine and reacted epoxy/Jeffamine mixtures.

RESULTS AND DISCUSSION

GPC characterization of the *in situ* reaction

The reaction of epoxide group with amine is fundamental for curing epoxy resins. However, it is not clear if the specific conditions described in Experimental procedure are adequate to the *in situ* reaction formation of rubber nanoparticles. Gel permeation chromatography (GPC) can provide evidence for a new polymer production in a chemical reaction by detecting molecular weight. When a dilute polymer solution runs through GPC, the highest molecular weight fraction always comes out first, corresponding to the shortest retention time, and then lower molecular weight fraction flows out, relating to longer retention time.

Two samples were prepared for GPC. One is the unreacted epoxy/Jeffamine, prepared by physical mixing and then freeze-stored until use; the other is the reacted epoxy/Jeffamine, prepared as in Experimental Figure 2 is the GPC chromatographs of the two samples. For the unreacted epoxy/Jeffamine mixture, two peaks were expected for epoxy and Jeffamine, respectively, which are confirmed in Figure 2. Regarding the reacted epoxy/Jeffamine mixture, a new peak was expected for a new polymer produced by the reaction of epoxy and Jeffamine, apart from the former two peaks. In Figure 2, a new peak indeed appears at a shorter retention time 1900 s, meaning a higher molecular weight for a new polymer. This evidenced the reaction of epoxy and Jeffamine for the formation of rubber nanoparticle.

^1H NMR characterization of the *in situ* reaction

The Jeffamine D2000 molecular formula and the reactions between epoxy and Jeffamine are shown in

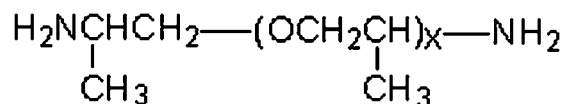


Figure 3 Structure of Jeffamine.

Figures 3 and 4, respectively. Figure 5 shows the ^1H NMR spectra of the unreacted and reacted epoxy/Jeffamine. In the mixture of unreacted epoxy/Jeffamine, the $-\text{CH}-$ proton adjacent to the amine exhibits a broad resonance at 2.05 ppm. Upon reaction of the amine to the epoxide ring, the resonance of the $-\text{CH}-$ proton would disappear or chemically shift. The ^1H NMR spectra for the reacted mixture shows no peak at 2.05 ppm, while a new resonance appeared at 2.16 ppm might be the shifted peak or the resonance caused by the residue of the solvent acetone. This result provides a supplementary proof to the GPC evidence for the reaction between the epoxide and the amine.

Microstructure characterization by TEM

The sample of epoxy/rubber nanocomposite containing 15 wt % rubber was cryo-sectioned and observed with TEM, as shown in Figure 6. Nothing was observed at low magnification. In Figure 6(a), however, fine particles were observed at a magnification 2.3×10^5 . Higher magnification microphotograph in Figure 6(b) demonstrates that the diameter of these particles is 2–3 nm and the dispersion is fine.

Jeffamine D2000 is widely used as a hardener for epoxy. But it plays the role of *in situ* formed rubber nanoparticles in this study. The foregoing GPC, NMR, and TEM analysis demonstrates that the nanoparticles were formed *in situ* by the reaction of Jeffamine D2000 with epoxy. Thus, the reaction degree may be high. As the nanoparticles were formed by chemical bonding and all reactive sites were consumed, they are thermally stable.

Mechanical properties of epoxy/rubber nanocomposites

Liquid rubber is the conventional toughener for epoxy. It is compatible with epoxy at processing temperatures (i.e., 100–120°C), while phase separation

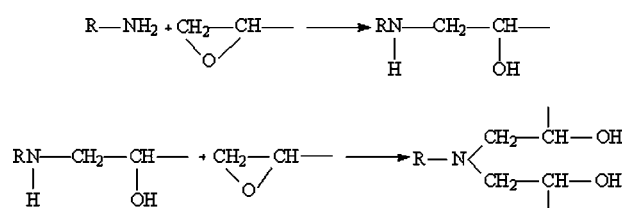


Figure 4 Reactions of epoxy with Jeffamine.

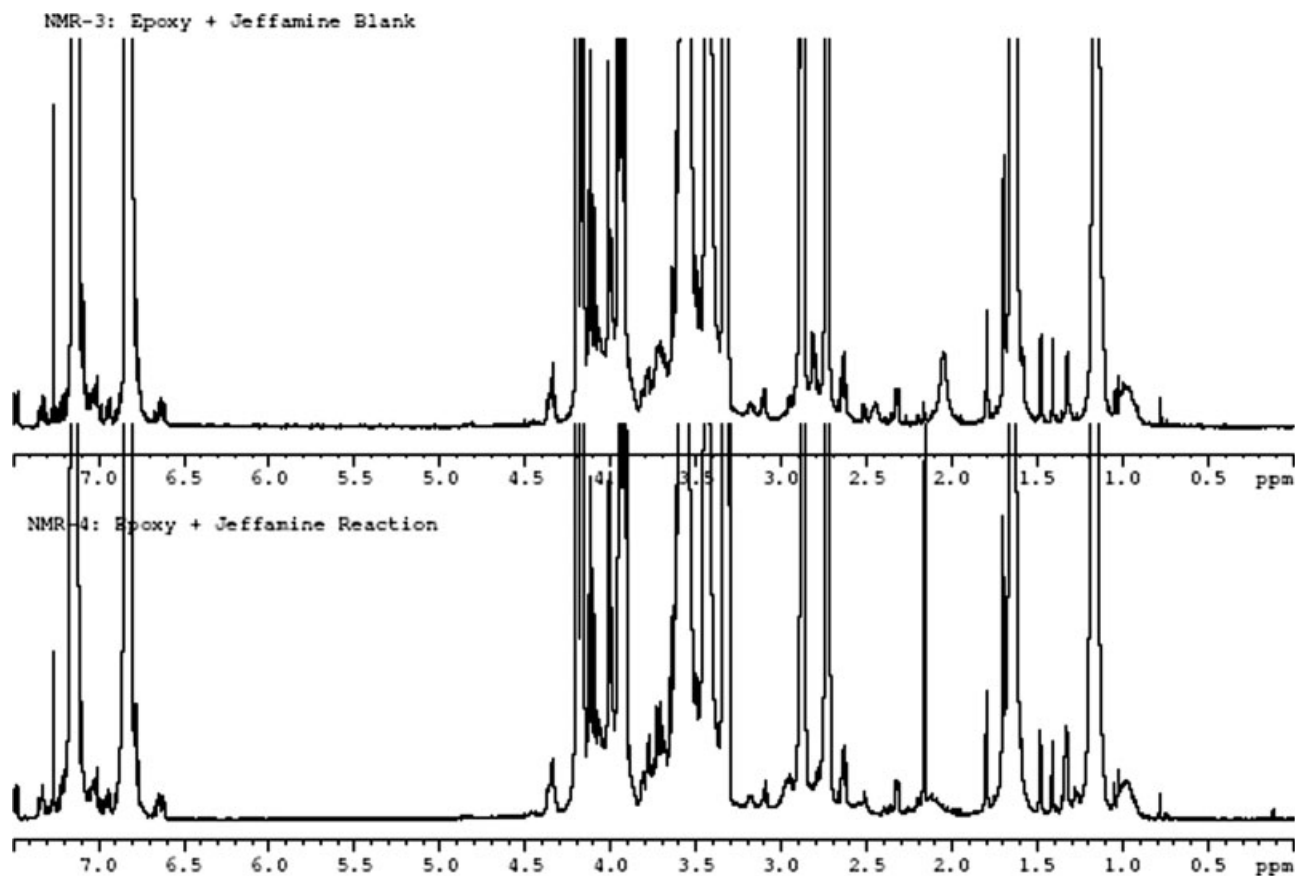


Figure 5 HNMR spectra of unreacted epoxy/Jeffamine and reacted epoxy/Jeffamine.

occurs during crosslinking. As a result, rubber particles with diameters of 0.1–10 μm are formed. The low Young's modulus, microscale size, and poor interface of the particles induced a serious reduction of the matrix modulus. There are 12.2 and 26.3% decrease of Young's modulus with the addition of 10 and 15 wt % rubber, respectively.²⁰

Table I lists the comprehensive properties of epoxy/rubber nanocomposites. With increase of the nanoparticle content, the modulus has no obvious change until over 10 wt % rubber. The Young's modulus decreases only 12.6% with 15 wt % rubber nanoparticles. The much smaller modulus decrease differentiates the nanoparticle effect from the microparticle effect. The most obvious characteristic of nanoparticles is their high specific surface area and particle amount in comparison with microparticles. When tensile-deformed, therefore, these nanoparticles would constrain matrix deformation more efficiently, leading to a fairly smaller reduction of Young's modulus.

With increase of the nanoparticle content, the tensile strength drops obviously. It decreases 12.9% and 23.7% with 10 and 15 wt % rubber nanoparticles, respectively. In comparison, the tensile strength

decreases 13.9% and 29.6% with 10 and 15 wt % liquid rubber microparticles, respectively.²⁰ It means there is no size-induced effect on tensile strength, as different to modulus.

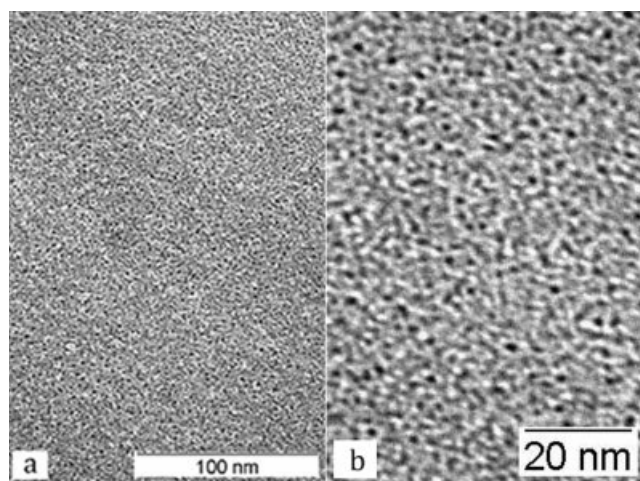


Figure 6 TEM images of the epoxy/rubber nanocomposite containing 15 wt % rubber: (a) at 230×10^3 magnification; (b) at 660×10^3 magnification.

TABLE I
Mechanical Properties and Toughness of Epoxy/Rubber Nanocomposite

Materials	Young's modulus (GPa)	Tensile strength (MPa)	Elongation at yield (%)	Plane-strain fracture toughness (K_{Ic} , MPa m ^{1/2})	Critical strain energy release rate (G_{Ic} , kJ/m ²)
Epoxy	2.85 ± 0.21	66.9 ± 0.73	4.75 ± 0.04	0.67 ± 0.01	0.14 ± 0.03
Epoxy/Jeff, 5 wt %	2.89 ± 0.07	68.9 ± 0.23	4.41 ± 0.08	1.00 ± 0.04	0.30 ± 0.02
Epoxy/Jeff, 10 wt %	2.90 ± 0.30	58.3 ± 0.14	3.82 ± 0.14	1.26 ± 0.02	0.49 ± 0.02
Epoxy/Jeff, 15 wt %	2.49 ± 0.18	54.3 ± 0.21	3.65 ± 0.05	1.53 ± 0.06	0.84 ± 0.07

Toughness of epoxy/rubber nanocomposites

Tapping is a well-known procedure to initiate a sufficiently sharp crack, but a crack made by tapping is not necessarily sufficiently sharp. Our research demonstrates only an instantly propagated crack is a sufficiently sharp crack. Unfortunately, many publications lack of details of crack preparation, which may result in inaccurate toughness data. Thus, we just compared our results with the conventional epoxy/rubber composite reported by Xiao and Ye,²⁰ who adopted the same procedure of material preparation and testing as this study.

In Table I, the fracture toughness of the nanocomposites exhibits a linear increase with the rubber nanoparticle content. With 10 wt % nanoparticle content, the toughness increases 88.1% in comparison with 80.6% by the same fraction of liquid rubber microparticles.²⁰ The critical strain energy release rate exhibits a similar improvement. This means the rubber nanoparticles toughen epoxy similarly as the conventional rubber microparticles. But it is noteworthy that there is no modulus deterioration with 10 wt % nanorubber.

Fracture mechanisms of epoxy/rubber nanocomposites

The principal toughening mechanism of liquid rubber toughened epoxy was shown to involve internal cavitation of the rubber particles and the subsequent formation of shear bands. In comparison with the conventional rubber microparticles, the rubber nanoparticles achieve similar toughening effect but with much smaller modulus deterioration. So what is the toughening mechanism for the 2–3 nm rubber particles?

Sub-surface analysis of critically fractured CT specimens

Brittle epoxy is strain and orientation-free; it refracts light equally in all directions and is optically isotropic. Plastically deformed polymers are not optically isotropic and therefore are birefringent. Birefringence can be used to detect residual elastic and plastic strains in toughened epoxy.²⁵ Optically iso-

tropic, stress-free materials will appear dark when viewed between completely crossed polarizers, while deformed toughened epoxy is birefringent and transmit part of the light. A quarter wave plate was inserted in the light path to shift the color of the image and to provide isometric fringes.

Figure 7(a) is an optical micrograph of the thin section taken in the mid-plane and near the crack tip of a neat epoxy CT specimen. This micrograph contains the crack which was unloaded at the subcritical

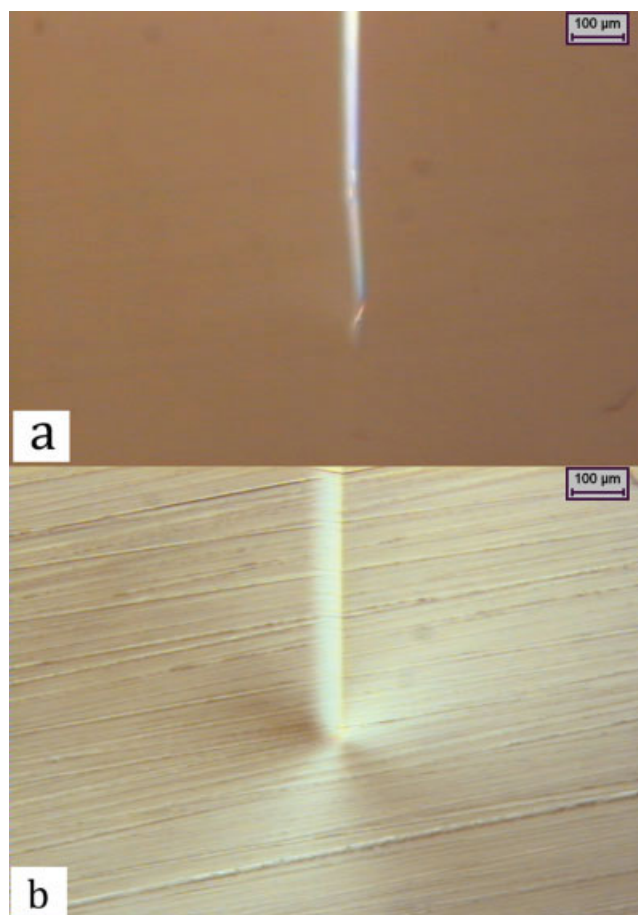


Figure 7 Optical micrograph of a thin section taken mid-plane and near the arrested crack tip of (a) the neat epoxy CT under crossed-polars; and (b) the CT sample containing 15 wt % rubber nanoparticles under crossed-polars. [Color figure can be viewed in the online issue, which is available at www.interscience.wiley.com.]

loading. There is no evidence of any birefringent characteristics, implying no plastic deformation in the vicinity of the crack tip. The absence of a plastic zone correlates well with the low critical stress intensity value measured.

Figure 7(b) contains an optical micrograph of a thin section taken in the mid-plane and near the crack tip for an epoxy modified with 15 wt % rubber nanoparticles. There is an obvious birefringent zone at the crack tip, indicating plastic deformation in the vicinity of the crack tip, in correspondence with the 500% enhanced energy release rate. This means the rubber nanoparticles are able to promote or induce the matrix plastic deformation.

Subsurface analysis of fractured tensile specimens

Figure 8(a) is an optical micrograph of a thin section taken parallel to the tensile direction and near the fractured region of the neat epoxy tensile sample. This section is viewed using crossed-polarized light with a quarter wave plate. There is no evidence of any birefringent characteristics. It reveals that there is no plastic deformation for the tensile fracture sample.

Figure 8(b) contains an optical micrograph of a thin section taken parallel to the tensile direction and near the necked region of the tensile sample containing 15 wt % rubber nanoparticles. A bright but diffuse shear yielded zone was observed, indicating plastic deformation in the vicinity of tensile fractured sample. This may show that the rubber nanoparticles plasticize the epoxy, corresponding to the decreased tensile strength.

TEM analysis of critically fractured CT specimens

The principal toughening mechanism of the conventional liquid rubber-modified epoxy is generally regarded as the internal cavitation of the rubber particles and the subsequent formation of shear bands.²³ In addition, evidence for other mechanisms such as crack deflection and particle bridging was reported.²⁵

According to the foregoing OM analysis, the main toughening mechanism of the epoxy/rubber nanocomposite is with the enhanced plastic work at the crack tip caused by the matrix stress relaxation due to rubber nanoparticles. We employed TEM to search evidence for other mechanisms such as crack deflection and particle bridging. What we observed is similar to Figure 6: there is no particle cavitation or deformation; neither crack deflection or particle bridging is observed. This indicates the rubber nanoparticles are unable to cavitate, deflect crack, and bridge the crack faces. The matrix stress relaxation by the nanoparticles may be the sole toughening mechanism. This conclusion is supported by Yang

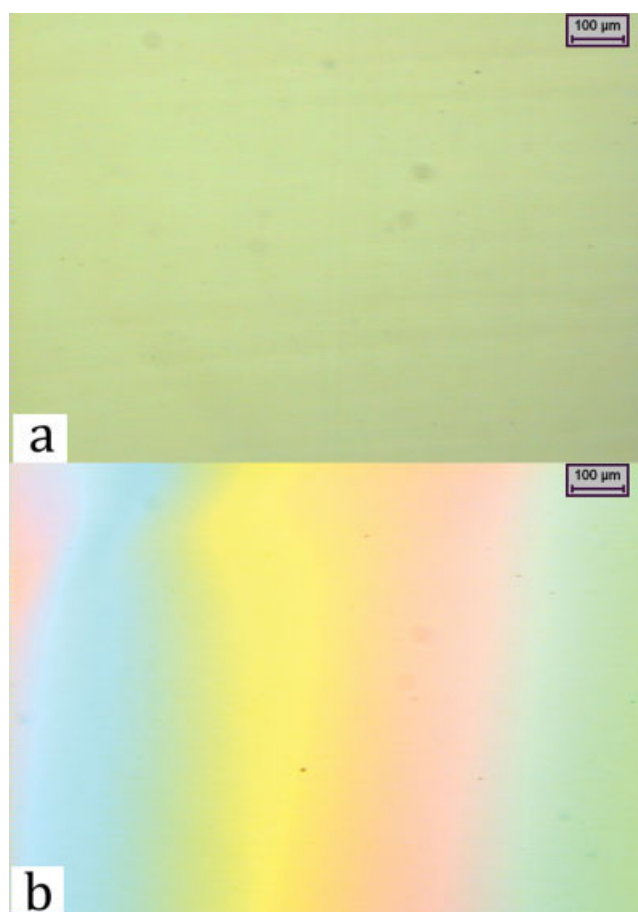


Figure 8 Optical micrograph under crossed-polars of a thin section taken parallel to the tensile direction and near the fractured region of (a) the neat epoxy CT under crossed-polars; and (b) the CT sample containing 15 wt % rubber nanoparticles under crossed-polars. [Color figure can be viewed in the online issue, which is available at www.interscience.wiley.com.]

et al.²⁶ The authors used Jeffamine D-230 and D-400 to simultaneously strengthen and toughen epoxy; the fracture mechanism was attributed to the reduction of internal stress due to the stress relaxation by the flexible molecular chains of the amines.

Rheological property of the epoxy/rubber nanocomposite

Rheology deals with the relationships between forces (stresses) and deformations of materials bodies. Most polymeric materials exhibit the combined properties of both liquid and solid, called viscoelasticity, a combination of the viscosity of a liquid and the elasticity of a solid. Compared to simple liquids, polymers are very different and have extremely high viscosity and a special flow characteristic, which is termed "non-Newtonian."²⁷ Here, we analysis the rheology of neat epoxy and the epoxy containing 15 wt % rubber nanoparticles at 100°C.

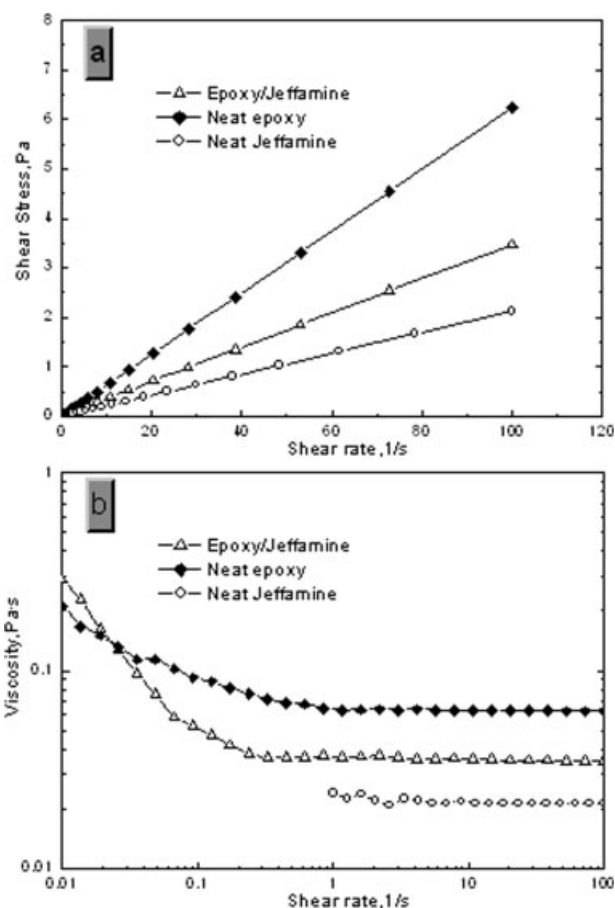


Figure 9 Rheology of neat epoxy and the epoxy containing 15 wt % rubber nanoparticles: (a) dependence to shear stress on shear rate; and (b) dependence of viscosity on shear rate.

Figure 9(a) contains the dependence of the shear stress on the shear rate for neat epoxy and epoxy/rubber nanocomposite before crosslinking. With increasing the shear rate, the shear stresses of both materials increase linearly, indicating Newtonian liquid behavior; upon the same shear rate, the nanocomposite shows a higher shear stress rate, as the nanoparticles enhance viscosity. In contrast, the liquid rubber-modified epoxy shows much higher slope of stress-rate and a shear-thinning (pseudoplastic) liquid behavior.²⁶ This means the epoxy/rubber nanocomposite is more readily for processing than the conventional epoxy/liquid rubber composite.

Figure 9(b) contains the dependence of the viscosity on the shear rate for neat epoxy and epoxy/rubber nanocomposite before crosslinking. The viscosity of the epoxy/rubber is obviously higher than neat epoxy and Jeffamine, and this means the reaction of epoxy and Jeffamine, supplementary evidence to NMR and GPC. With increasing the shear rate, the viscosities of the neat epoxy and the epoxy containing 15 wt % rubber nanoparticles decrease first and then stabilize the shear rate of 0.3 and 1.1 s⁻¹,

respectively. This is explained by the evolution of epoxy molecules with shear rate increase. At the beginning of viscosity measurement, epoxy molecules physically entangled each other and thus indicated highest viscosity. With increase of the shear rate, the molecules began to disentangle leading to reduced viscosity. The disentanglement tended to complete at a specific shear rate and since then the viscosity remained constant. It is noteworthy that the initial viscosity of the epoxy/rubber nanoparticle compound is lower than that for neat epoxy, in comparison with a higher viscosity of the compound at a higher shear rate. This is explained below. The rubber nanoparticles were formed by Jeffamine D-2000. As the Jeffamine chain is much more flexible than epoxy molecules, it may fold to form nanoparticles in epoxy. These nanoparticles thus may act as lubricators at low shear rate, indicating low viscosity. Increase of shear rate means higher load applied to the nanoparticles, which defolded the Jeffamine chains. Given that the graft reaction between the Jeffamine and epoxy, these defolded Jeffamine chains can increase viscosity obviously. The low viscosity at low shear rate may be useful in epoxy adhesive and coating industries.

CONCLUSION

We synthesised epoxy/rubber nanocomposite, investigated the mechanical properties and toughness, identified the toughening mechanism, and analyzed the rheology property. The *in situ* reaction was verified by GPC and ¹HNMR; the morphology was proved by TEM. In comparison with conventional liquid rubber, the nanocomposite containing 15 wt % nanoparticles achieves similar toughening effect with much less modulus deterioration. There is no effect of particle size on the tensile strength. The toughening mechanism was identified as the increased plastic work enabled by the stress relaxation of the matrix epoxy by the rubber nanoparticles; there are no particle cavitation or deformation; neither crack deflection or particle bridging were observed. The compound containing rubber nanoparticles shows lower initial viscosity at low shear rate in comparison with neat epoxy.

J.M. thanks the Australian Research Council (ARC) for the award of an Australian Postdoctoral Fellowship, tenable at the University of South Australia. J.M. appreciates GPC measurement by M. Siau. Jeffamine D-2000 was kindly provided by Huntsman Chemical Co., Singapore. The authors thank Prof Yiu-Wing Mai of USyd for useful comments and suggestions.

References

- Sultan, J. N.; Laible, R. C.; MacGarry, F. J. *Appl Polym Symp* 1971, 16, 127.

2. Hodgkin, J. H.; Simon, G. P.; Varley, R. J. *Polym Adv Technol* 1998, 9, 3.
3. Mezzenga, R.; Boogh, L.; Manson, J. A. *Compos Sci Technol* 2001, 61, 787.
4. Garg, A. C.; Mai, Y. W. *Compos Sci Technol* 1988, 31, 179.
5. Bagheri, R.; Pearson, R. A. *Polymer* 2000, 41, 269.
6. Sritama, K.; Ajit, K. *J Appl Polym Sci* 2005, 96, 2446.
7. Cao, Y. M.; Shao, Y. F.; Sun, J. *J Appl Polym Sci* 2003, 90, 3384.
8. Blanco, I.; Cicala, G.; Faro, C. L.; Recca, A. *J Appl Polym Sci* 2003, 89, 268.
9. Saxena, A.; Francis, B.; Rao, V. L.; Ninan, K. N. *J Appl Polym Sci* 2007, 106, 1318.
10. Ramakrishna, H. V.; Priya, S. P.; Rai, S. K. *J Appl Polym Sci* 2007, 104, 171.
11. Rosso, P.; Ye, L.; Friedrich, K.; Sprenger, S. *J Appl Polym Sci* 2006, 100, 1849.
12. Zhang, K. L.; Wang, L. X.; Wang, F.; Wang, G. J.; Li, Z. B. *J Appl Polym Sci* 2004, 91, 2649.
13. Ma, J.; Yu, Z. Z.; Zhang, Q. X.; Xie, X. L.; Mai, Y. W.; Luck, I. *Chem Mater* 2004, 16, 757.
14. Day, R. J.; Lovell, P. A.; Wazzan, A. A. *Compos Sci Technol* 2001, 61, 41.
15. Nagendiran, S.; Premkumar, S.; Alagar, M. *J Appl Polym Sci* 2007, 106, 1263.
16. Kim, N. H.; Kim, H. S. *J Appl Polym Sci* 2006, 100, 4470.
17. Ratna, D.; Varley, R.; Simon, G. P. *J Appl Polym Sci* 2003, 89, 2339.
18. Komarneni, S. *J Mater Chem* 1992, 2, 1219.
19. Ma, J.; Mo, M. S.; Du, X. S.; Rosso, P.; Friedrich, K.; Kuan, H. C. *Polymer*. Doi: 10.1016/j.polymer.2008.05.043.
20. Xiao, K. Q.; Ye, L. *J Mater Sci* 1998, 33, 2831.
21. Yu, S. R.; Hua, H. X.; Ma, J.; Yin, J. *Tribology International*. Doi: 10.1016/j.triboint.2008.03.001.
22. Ma, J.; Qi, Q.; Du, X. S.; Mo, M. S.; Zhang, L. Q. *Polym Test* 2007, 26, 262.
23. Yee, A. F.; Pearson, R. A. *J Mater Sci* 1986, 21, 2462.
24. Holik, A. S.; Kambrou, R. R.; Hobbs, S. Y.; Fink, D. G. *Microstruct Sci* 1979, 357, 7.
25. Pearson, R. A.; Yee, A. F. *J Mater Sci* 1991, 26, 3828.
26. Yang, G.; Fu, S. Y.; Yang, J. P. *Polymer* 2007, 48, 302.
27. Han, C. D. *Rheology in Polymer Processing*; Academic Press: New York, 1976.
28. Sritama, K.; Ajit, K. *J Appl Polym Sci* 2005, 96, 2446.